Title

Ethylene controls cambium stem cell activity via promoting local auxin biosynthesis

Journal

New Phytologist, 239(3)

ISSN

0028-646X

Authors

Yu, Qin
Cheng, Chenxia
Zhou, Xiaofeng
et al.

Publication Date

2023-08-01

DOI

10.1111/nph.19004

Peer reviewed

New Phytologist

Research

Ethylene controls cambium stem cell activity via promoting local auxin biosynthesis

Qin Yu[1], Chenxia Cheng[1,2], Xiaofeng Zhou[1], Yonghong Li[3], Yingchun Hu[4], Chun Yang[1], Yingying Zhou[1], Tarek M. A. Soliman[5], Hao Zhang[6], Qigang Wang[6], Huichun Wang[6], Cai-Zhong Jiang[7,8], Su-Sheng Gan[9], Junping Gao[1] and Nan Ma[1]

[1]Beijing Key Laboratory of Development and Quality Control of Ornamental Crops, Department of Ornamental Horticulture, China Agricultural University, Beijing 100193, China; [2]College of Horticulture, Qingdao Agricultural University, Qingdao 266109, Shandong, China; [3]School of Applied Chemistry and Biotechnology, Shenzhen Polytechnic, Shenzhen 518055, Guangdong, China; [4]Core Facilities, College of Life Sciences, Peking University, Beijing 100871, China; [5]Faculty of Agriculture, New Valley University, New Valley Governorate 72511, New Valley, Egypt; [6]Flower Research Institute, Yunnan Academy of Agricultural Sciences, Kunming 650205, Yunnan, China; [7]Crop Pathology and Genetic Research Unit, United States Department of Agriculture, Agricultural Research Service, Davis, CA 95616, USA; [8]Department of Plant Sciences, University of California Davis, Davis, CA 95616, USA; [9]Plant Biology Section, School of Integrative Plant Science, College of Agriculture and Life Sciences, Cornell University, Ithaca, NY 14853, USA

Author for correspondence:
Nan Ma
Email: ma_nan@cau.edu.cn

Received: *19 January 2023*
Accepted: *26 April 2023*

New Phytologist (2023)
doi: 10.1111/nph.19004

Key words: auxin, cambium, ethylene, HD-ZIP I transcription factor, *Rosa hybrida*.

Summary

- The vascular cambium is the main secondary meristem in plants that produces secondary phloem (outside) and xylem (inside) on opposing sides of the cambium. The phytohormone ethylene has been implicated in vascular cambium activity, but the regulatory network underlying ethylene-mediated cambial activity remains to be elucidated.
- Here, we found that *PETAL MOVEMENT-RELATED PROTEIN1* (*RhPMP1*), an ethylene-inducible HOMEODOMAIN-LEUCINE ZIPPER I transcription factor in woody plant rose (*Rosa hybrida*), regulates local auxin biosynthesis and auxin transport to maintain cambial activity.
- Knockdown of *RhPMP1* resulted in smaller midveins and reduced auxin content, while *RhPMP1* overexpression resulted in larger midveins and increased auxin levels compared with the wild-type plants. Furthermore, we revealed that *Indole-3-pyruvate monooxygenase YUCCA 10* (*RhYUC10*) and *Auxin transporter-like protein 2* (*RhAUX2*), encoding an auxin biosynthetic enzyme and an auxin influx carrier, respectively, are direct downstream targets of RhPMP1.
- In summary, our results suggest that ethylene promotes an auxin maximum in the cambium adjacent to the xylem to maintain cambial activity.

Introduction

Unlike animals, plants can grow continuously and develop new tissues and/or organs to adapt the seasonal changes and various stimuli. The basis of this plastic growth mode is dependent on local stem cell niches at the apical or lateral meristem in the whole plant body (Love *et al.*, 2009). Apical meristems include the shoot apical meristem (SAM) and root apical meristem (RAM), which are responsible for the axial elongation (Etchells *et al.*, 2012). The vascular cambium is a lateral secondary meristem in plants. During secondary growth, cambial stem cells proliferate and subsequently differentiate into secondary phloem (outside) and xylem (inside) on opposing sides of the cambium in dicotyledonous species. These tissues form a complex system that not only transports water, nutrients, and phytohormones and peptide signaling molecules, but also provides mechanical support (Björklund *et al.*, 2007; Lucas *et al.*, 2013). Meanwhile, the activity of cambium is also closely related to plant regeneration process (Sugimoto *et al.*, 2010) and to regulate the plant dormancy and activity in response to seasons (Swarup *et al.*, 2007; Hu *et al.*, 2016). Thus, maintaining of cambium activity is an important biological event that enabling plants to remain self-renewing throughout their life cycle.

Proliferation and subsequent differentiation of cambium stem cells are tightly regulated by signaling factors, such as phytohormones, peptides, and mechanical signals (Hirakawa *et al.*, 2010; Oles *et al.*, 2017). Auxin is the predominant phytohormone involved in maintaining the activity of cambium stem cells (Mao *et al.*, 2016; Qin *et al.*, 2017). High levels of auxin-dependent activation of CLASS III HOMEODOMAIN-LEUCINE ZIPPER (HD-ZIP III) transcription factors promote xylem identity (Smetana *et al.*, 2019). Compared with auxin, the role of ethylene in regulating cambium activity is less known. In *Arabidopsis thaliana*, ethylene-induced cell division in the quiescent center (QC), a region of stem cells in the root (Ortega-Martinez *et al.*, 2007). In Arabidopsis (*Arabidopsis thaliana*), the ethylene-overproducing mutants *1-aminocyclopropane-1-carboxylate synthase 7* (*acs7-d*) and *ethylene overproducer 1* (*eto1*) exhibit

enhanced cambial activity (Yang *et al.*, 2020). Moreover, two ethylene response factors (ERFs), ERF018 and ERF109, act redundantly in a parallel pathway to CLV-3/ESR1-LIKE 41 (CLE41)-PHLOEM INTERCALATED WITH XYLEM (PXY) signaling to promote cell division in vascular meristems (Etchells *et al.*, 2012). In aspen (*Populus termula*), *ETHYLENE INSENSITIVE 3D* (*EIN3D*) and *ERFs* hub (*ERF118/119*) were involved in regulation of cambial growth and wood formation (Seyfferth *et al.*, 2018). In addition, ethylene has also been demonstrated to affect many characteristics of tension wood (TW) formation in hybrid aspen (Seyfferth *et al.*, 2019). To date, however, the underlying mechanism of ethylene in controlling cambium activity remains largely unknown.

High levels of exogenous ethylene (or ethylene precursors) affect cambial growth, xylem morphology, and ontogenesis of vessels, fibers, and rays during wood formation (Little & Savidge, 1987). These responses were demonstrated in hybrid aspen (*Populus tremula* × *tremuloides*; Love *et al.*, 2009). Several *ERFs* have been implicated in regulating cambium activity. In Arabidopsis, *ERF018* and *ERF109* are required for the increased cambial cell division observed in ethylene-overproducing *eto* mutants (Etchells *et al.*, 2012). Furthermore, overexpression of *ERF18*, *ERF34*, and *ERF35* increases the stem diameter (Vahala *et al.*, 2013). These studies suggest that ethylene is a key signal in regulating vascular stem cell activity; however, the specific molecular mechanism has not been characterized.

In this study, we investigated the role of ethylene in regulating vascular stem cell activity in a woody plant rose (*Rosa hybrida*). We determined that ethylene directs local auxin biosynthesis in the cambium in rose. Ethylene promoted the transcription of a HD-ZIP I transcription factor gene, *PETAL MOVEMENT-RELATED PROTEIN1* (*RhPMP1*). Knockdown of *RhPMP1* significantly reduced auxin levels in the cambium and resulted in severe defects in cambium cell activity and xylem development, while *RhPMP1* overexpression enhanced cambium activity. Furthermore, RhPMP1 directly activated the expression of *YUCCA 10* (*RhYUC10*) and *Auxin transporter-like protein 2* (*RhAUX2*), encoding an auxin biosynthetic enzyme and an auxin influx carrier, respectively, which generated an auxin maximum in the cambium adjacent to the xylem. We concluded that ethylene promotes cambium activity by activating local auxin biosynthesis.

Materials and Methods

Plant materials and growth condition

Rose (*Rosa hybrida*) cv Samantha plantlets were propagated by from tissue-cultured plants with same age. The first node from base was cut and cultured on Murashige and Skoog medium (Sigma) supplemented with 3% (m/v) sucrose, 1.0 mg l^{-1} 6-benzylaminopurine (6-BA), 0.05 mg l^{-1} α-naphthaleneacetic (NAA), and 1.0 mg l^{-1} gibberellic acid (GA_3) for 30 d at same conditions (22°C, 16 h : 8 h, light : dark). Thirty plantlets of each genotype (WT, *RhPMP1*-OE, and *RhPMP1*-RNAi) with the same growth potential were transferred to a rooting medium comprising ½-strength Murashige & Skoog medium supplemented with 3% (m/v) sucrose and 0.1 mg l^{-1} NAA for 30 d at same conditions (22°C, 16 h : 8 h, light : dark). The rooted plants were planted in plastic pots containing 1 : 1 (v/v) peat : vermiculite at 22 ± 1°C, relative humidity 60–70%, and a 16 h : 8 h, light : dark photoperiod.

After the plants were grown in a pot for 2 months, the leaf veins for section were sampled at 1 mm from the petiole in the tip leaflet of the third node, counting from the apical of WT, *RhPMP1*-OE, and *RhPMP1*-RNAi plants.

Rose transformation

The full-length *RhPMP1* coding sequence was inserted into the p*Super*1300-*GFP* vector to generate the p*Super*:*RhPMP1-GFP* overexpression vector. The amplified *RhPMP1* fragment was inversely inserted into the pFGC1008 vector to generate the *RhPMP1*-RNAi vector. Rose transformation was performed as described previously. Briefly, the p*Super*:*RhPMP1-GFP* overexpression vector and *RhPMP1*-RNAi vector were introduced into Agrobacterium (*Agrobacterium tumefaciens*) strain EHA105 and shaken overnight at 28°C until the bacterial OD_{600} = 0.6–0.8, and the bacteria were collected by centrifugation. Then, an equal volume of suspension buffer and suspended bacterium was mixed and incubated for 2 h at 28°C with shaking. Then, rose somatic embryos were immersed in the bacterial suspension and shaken for 40 min at 28°C. The somatic embryos were incubated for 3 d in the dark, cultured in a 16 h : 8 h, light : dark photoperiod. First, the somatic embryos were transferred to selective proliferation medium. After 2 months, the somatic embryos were transferred to selective germination medium, and finally to selective proliferation medium until the buds with anti-hygromycin B resistance were obtained, they were transferred to selective proliferation medium. After 1 month, the resistant seedlings were transferred to rooting medium. Rooted plants were transferred to a culture room with 22 ± 1°C. The primers used are listed in Supporting Information Table S1.

RNA extraction and reverse transcription quantitative PCR (RT-qPCR)

Total RNA from the tip leaflets at the third node, counting from the apical, was extracted using the hot borate method as described previously. Briefly, the leaves were ground with liquid nitrogen and preheated extraction buffer (200 mM sodium tetraborate decahydrate, 30 mM EGTA, 1% deoxycholic acid sodium salt, 10 mM dithiothreitol, 2% polyvinylpyrrolidone 40, and 1% Nonidet P-40) was added to the samples. RNA was precipitated using 2 M LiCl. Then, the pellet was dissolved in 1 M Tris–HCl (pH 7.5). RNA was reprecipitated with ethanol at −80°C for 2 h and dissolved in 30 µl RNA-free water.

For each sample, 1 µg DNase-treated RNA was used to synthesize first-strand cDNA with oligo d(T) or random primers and HiScript II Q RT SuperMix (Cat. R223-01; Vazyme, Nanjing, China). The resulting cDNA products were separated on a 1.2% agarose gel, and the images were scanned and analyzed using an AlphaImager 2200. Quantitative PCR

(qPCR) reactions (20 µl) were performed using 1 ml cDNA as template. The ABI Step One Plus Real-Time PCR system (Applied Biosystems, Waltham, MA, USA) and KAPA SYBR FAST Universal qRT-PCR Kit (Kapa Biosystems, Wilmington, MA, USA) were used for qPCR. The relative expression levels of genes were normalized to the reference gene *Ubiquitin 2* (*RhUBI2*) and calculated using the $2^{-\Delta\Delta C_t}$ method. All reactions were performed with at least three biological replicates. The primers are listed in Table S1.

Histochemical staining of GUS activity

To monitor the activity of the *GUS* reporter gene, tissues were submerged in a staining solution containing 0.5 mg ml^{-1} 5-bromo-4-chloro-3-indolyl-b-D-glucuronic acid (X-Gluc) with 100 mM sodium phosphate (pH 7.0), 10 mM EDTA, 0.01% Triton X-100, 5 mM potassium ferricyanide ($K_3Fe(CN)_6$), and potassium ferrocyanide ($K_4Fe(CN)_6$) and incubated for 12 h at 37°C in the dark (Hemerly *et al.*, 1993; Hur *et al.*, 2015). After staining, plant tissues were cleared by immersing them in 70% ethanol.

Yeast one-hybrid assays

For the yeast one-hybrid assays, the full-length *RhPMP1* coding sequence was amplified and cloned into prey vector pB42AD. The promoters of *RhIAA32*, *RhAUX2*, *RhSAUR15*, and *RhYUC10* were inserted into the *pLacZi* vector. The constructed plasmids and empty vectors were transformed into yeast strain EGY48. The transformants were cultivated on SD/-Trp/-Ura medium and tested on SD/-Trp/-Ura medium with 5-bromo-4-chloro3-indolyl-b-D-galactopyranoside. The primers are listed in Table S1.

Electrophoretic mobility shift assays (EMSA)

The construct encoding the full-length RhPMP1 protein sequence was fused with the glutathione S-transferase (GST) tag and introduced into *Escherichia coli* strain BL21 (DE3). The RhPMP1-GST recombinant proteins were produced using 0.2 mM isopropyl β-D-1-thiogalactopyranoside (IPTG) at 28°C for 10 h. The recombinant proteins were affinity-purified using glutathione sepharose 4B (GE Healthcare, Chicago, IL, USA). Probes of *c.* 45 bp in length containing the binding site of the *RhYUC10* promoter were synthesized and labeled with biotin at their 5′ end, unlabeled probe as competitor was added to the reactions. EMSA was performed using the Light Shift Chemiluminescent EMSA Kit (Thermo Fisher Scientific, Waltham, MA, USA). The primers are listed in Table S1.

Chromatin immunoprecipitation (ChIP)-qPCR assay

The ChIP-qPCR assay was performed as described previously. Petals of transgenic lines overexpressing *RhPMP1-GFP* were used in the assay. For ChIP, 2 g of petals was harvested and ground in liquid nitrogen. The powder was resuspended in buffer (10 mM Tris–HCl, pH 8.0, 0.4 M sucrose, 1 mM $MgCl_2$, 1 mM $CaCl_2$, 1% Triton X-100, 0.5% PVP40, 1 mM DTT, 0.1 mM PMSF, and EDTA-Free cOmplete™ Protease Inhibitor Cocktail (Sigma-Aldrich)) and cross-linked using 1% (v/v) formaldehyde and incubated for 10 min at 4°C. The powder was incubated with 0.15 M glycine for 5 min at 4°C to quench the formaldehyde. The chromatin was subsequently isolated and sonicated to produce DNA fragments. Anti-GFP (AE012; ABclonal, Wuhan, China) was used for ChIP analysis. The co-precipitated DNA products were purified and analyzed by qPCR. All primers used for ChIP assays are listed in Table S1.

Dual Luciferase (LUC)/Renilla luciferase (REN) reporter assay

The full-length *RhPMP1* coding sequence was cloned into the pGreenII 62-SK vector to generate Pro35S:*RhPMP1* effector constructs. The promoters of *RhYUC10*, *RhAUX2*, and *RhSAUR15* were cloned into pGreenII 0800-LUC reporter constructs. The constructs were introduced into Agrobacterium strain GV3101 harboring the pSoup plasmid. Cultures containing the respective constructs were incubated overnight and collected by centrifugation and resuspended in infiltration buffer (10 mM MgCl2, 0.2 mM acetosyringone, and 10 mM MES, pH 5.6) to a final OD_{600} of 1.0. The reporters and effectors were transiently transformed into *Nicotiana benthamiana* leaves. After 3 d infiltration, 1 mM luciferin was sprayed onto *N. benthamiana* leaves and luminescence was detected using an automatic chemiluminescence image analysis system. The luciferase activity was determined using a Luciferase Assay System Kit (Promega). The primer sequences used are listed in Table S1.

In situ hybridization

In situ hybridization of leaf midvein and stem was performed as described previously (Cheng *et al.*, 2021). Briefly, the leaf midvein tissues were fixed in 4% (w/v) paraformaldehyde by vacuum infiltration for 25 min and gently shaken overnight at 4°C. The samples were dehydrated in a graded ethanol series and embedded in Paraplast plus (Sigma). Sense and antisense probes of RhPMP1, RhYUC10, RhAUX2, RhARF5, and RhWOX4 were synthesized and labeled using a DIG-RNA labeling Kit (Roche). Microtome sections (8–10 µm) were applied to RNase-free slides and incubated with DIG-labeled sense or antisense probes overnight at 55°C. Hybridizations were visualized using nitroblue tetrazolium/5-bromo-4-chloro-3-indolyl phosphate stock solution (Roche) and photographed with an optical microscope (Olympus BH-2, Tokyo, Japan). The primers are listed in Table S1.

Histological analyses

Semi-thin sectioning of petal base and leaf midvein was carried out as described previously (Cheng *et al.*, 2021). Briefly, petal and leaf tissues were fixed in 2.5% glutaraldehyde. Samples were embedded in Low Viscosity Embedding Kit (Spurr; EMS,

Hatfield, PA, USA) resin (EMS) and sectioned at 3 µm with a Leica RM2265 rotary microtome (Leica Microsystems, Wetzlar, Germany). Thin sections were stained with 0.02% toluidine blue in 100 mM phosphate buffer (pH 7.2). Slides were observed using an optical microscope (Olympus BH-2).

Measuring endogenous auxin content

Endogenous auxin contents were measured by an ultra-performance liquid chromatography–tandem mass spectrometry (UPLC-MS/MS) system. Around 50 mg of leaf midvein was harvested from WT, *RhPMP1*-OE, and *RhPMP1*-RNAi plants and immediately ground into powder in liquid nitrogen. Samples were extracted by pre-cooled buffer (IPA : H_2O : HCl = 2 : 1 : 0.002) containing internal standards and dipped into cold $CHCl_3$ for 30 min at 4°C. After centrifuging at 12 000 ***g*** at 4°C for 15 min, the supernatants were dried with a nitrogen gas stream and then dissolved with methyl alcohol. The new supernatant concentration was detected by UPLC-MS/MS. Each sample was performed in three biological replicates.

Immunolocalization of indole acetic acid

Immunolocalization of indole acetic acid (IAA) was performed as described previously (Liang *et al.*, 2020; Nie *et al.*, 2021). Briefly, the leaf vein was cross-linked in pre-cooled 3% (w/v) 1-(3-Dimethylaminopropyl)-3-ethylcarbodiimide hydrochloride (EDC; Sigma-Aldrich) for 1 h in a dark chamber and transferred to 4% (w/v) paraformaldehyde and 2% glutaraldehyde for overnight at 4°C. The samples were dehydrated in a graded ethanol series and embedded in Paraplast (Sigma), and sectioned at 8–10 µm with a Leica RM2265 rotary microtome (Leica Microsystems). The slides were subsequently incubated in 10 mM PBS containing 0.1% (v/v) Tween 20, 1.5% (v/v) Glycine, and 5% (w/v) bovine serum albumin (BSA) for 2 h at 37°C. Anti-IAA polyclonal antibody (Agrisera, Vännäs, Sweden) was applied to each slide and incubated overnight in a humidity chamber at 4°C, and then ABflo™ 488-labeled anti-rabbit IgG antibody was placed on each slide and incubated for 4 h in a humidity chamber at room temperature. After washing with 10 mM PBS three times for 15 min each, specimens were mounted with an anti-fade reagent and observed with a confocal laser-scanning microscope (Zeiss LSM 800).

1-Aminocyclopropane-1-carboxylic acid treatment

The 1-aminocyclopropane-1-carboxylic acid (ACC) treatment was performed as described previously (Vahala *et al.*, 2013). Tissue-cultured seedlings of WT and *RhPMP1*-RNAi plants were treated with ACC or water (control). The ACC solution was added to the surface of the tissue culture medium to achieve a final concentration of 100 µM ACC in the medium after diffusion. For controls, the same volume of sterile-filtered deionized water was applied without ACC. The first newly formed internodes at 15 d after ACC or water treatment were collected for sectioning, *in situ* hybridization, and immunofluorescence analysis.

Results

An ethylene-inducible HD-ZIP I transcription factor RhPMP1 is dispensable for maintaining cambial cell activity

Auxin has a pivotal role in regulating cambium activity in plants. Ethylene also has been implicated in promoting cambium activity (Love *et al.*, 2009; Etchells *et al.*, 2012), though its regulatory pathway is not known. We previously reported that *RhPMP1*, encoding an ethylene-induced HD-ZIP I transcription factor, controls flower opening by regulating cell endoreduplication in rose (Cheng *et al.*, 2021). In addition, we found the vascular size of *RhPMP1*-RNAi plants was smaller than that of the WT plants after ethylene treatment. Moreover, *RhPMP1* homologous gene, *Arabidopsis thaliana homeobox 12* (*ATHB12*), has been shown to regulate size and venation patterning in Arabidopsis leaves (Hur *et al.*, 2015; Moreno *et al.*, 2018). We thus speculated that RhPMP1 mediates the effects of ethylene on the development of vascular bundles in rose. β-Glucuronidase (GUS) staining revealed that the *RhPMP1* promoter was activated in leaf petioles, sepals, and the joint area of siliques, as well as the midvein of older leaves (Fig. S1). To further confirm *RhPMP1* function in vascular development, we generated *RhPMP1*-OE plants by agrobacterium-mediated transformation. Seven *RhPMP1*-OE transgenic lines were obtained and two representative lines (*RhPMP1*-OE#5 and *RhPMP1*-OE#7) were selected for further analyses (Fig. S2). The qRT-PCR result indicated that the expression levels of *RhPMP1* in the *RhPMP1*-OE #5 and #7were significantly higher than that of wild-type (WT; Fig. 1a). *RhPMP1*-RNAi transgenic lines have been obtained from our previous study (Cheng *et al.*, 2021), and we used the same *RhPMP1*-RNAi transgenic lines (*RhPMP1*-RNAi #2, *RhPMP1*-RNAi #4) in this study. *In situ* hybridization further showed that *RhPMP1* transcripts accumulated throughout the leaf midveins near the petiole (Fig. 1b). Silencing of *RhPMP1* using RNA interference (RNAi) significantly reduced the size of vascular bundles (VBs) in petioles, with fewer cells in the xylem (−31.1% for RNAi #2, −40.1% for RNAi #4), cambium (−16.4% for RNAi #2, −29.5% for RNAi #4), and phloem (−22.3% for RNAi #2, −18.6% for RNAi #4; Fig. 1c–g). Moreover, the *RhPMP1*-RNAi line had significantly smaller xylem cells than the WT (−45.5% for RNAi #2, −54.5% for RNAi #4; Fig. 1h). On the contrary, overexpressing *RhPMP1* dramatically enhanced VB development compared with the WT, notably in increased cell numbers in the cambium (+35.8% for OE #5 and +45.1% for OE #7) and xylem (+18.5% for OE #5 and +23.6% for OE #7), as well as enlarged xylem cells area (+42.1% for OE #5 and +50.0% for OE #7). We observed similar phenomena in the VBs of petals (Fig. S3a). *RhPMP1* overexpression also increased the number of vascular cells and the size of xylem cells (Fig. S3b–f), suggesting that the role of *RhPMP1* in regulating VB development is conserved in different organs.

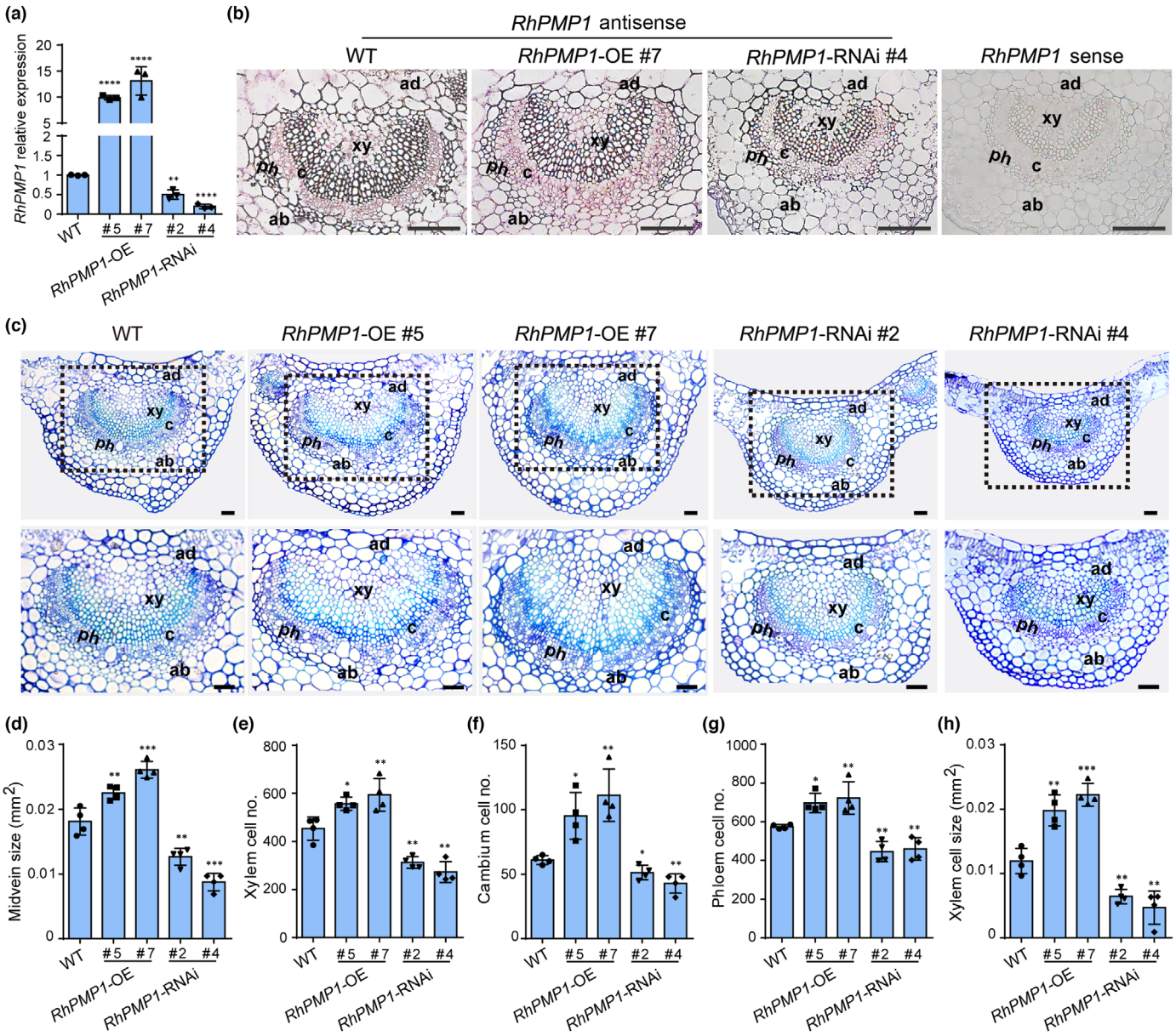

Fig. 1 Histological characterization leaf veins of *RhPMP1*-OE and *RhPMP1*-RNAi lines. (a) Quantitative real-time PCR (qRT-PCR) analysis of *RhPMP1* expression in WT plants, *RhPMP1*-OE (#5 and #7) and *RhPMP1*-RNAi (#2 and #4). Values are means ± SD ($n = 3$). (b) *In situ* hybridization of *RhPMP1* in the leaf midvein 1 mm from the petiole in the tip of the leaflet of the third node, counting from the apical of WT, *RhPMP1*-OE, and *RhPMP1*-RNAi plants. Plants were grown in potting soil for 2 months. The *RhPMP1* sense probe was used as the negative control. Bars, 100 µm. (c) Histological analysis of leaf midveins of the WT and the *RhPMP1*-OE (#5 and #7) and *RhPMP1*-RNAi (#2 and #4) lines. Transverse sections were taken from the midvein of the leaf 1 mm from the petiole in the tip of leaflet of the third node, counting from the apical of WT, *RhPMP1*-OE, and *RhPMP1*-RNAi plants. Plants were grown in potting soil for 2 months. Lower panels show the enlarged areas marked in the upper panels. Bar, 50 µm. (d–h) Midvein size (d); cell number of the xylem (e), cambium (f), and phloem (g); and xylem cell size (h) of WT, *RhPMP1*-OE, and *RhPMP1*-RNAi plants, respectively. Values are mean ± SD ($n = 4$). ad, adaxial side; ab, abaxial side; c, cambium; xy, xylem; ph, phloem. Asterisks indicate statistically significant differences (Student's *t*-test: *, $P < 0.05$; **, $P < 0.01$; ***, $P < 0.001$; ****, $P < 0.0001$).

RhPMP1 broadens and enhances the auxin maximum in the cambium adjacent to the xylem by directly activating *RhYUC10* and *RhAUX2* expression

To investigate how RhPMP1 controls VB development, we conducted a transcriptome analysis using WT and *RhPMP1*-OE #7 plants. Compared with the WT, we identified 1389 upregulated and 948 downregulated genes in the *RhPMP1*-OE line (Table S2) using a false discovery rate (FDR) of 0.05 and a fold change of at least two as selection criteria. Kyoto Encyclopedia of Genes and Genomes (KEGG) analysis of the differentially expressed genes (DEGs) in the WT vs *RhPMP1*-OE indicated that the term of 'plant hormone signal transduction' was significantly enriched. In addition, some pathways were related to thickening of

secondary cell walls, such as 'phenylpropanoid biosynthesis' term was enriched, consistent with the enhanced xylem phenotype in the *RhPMP1*-OE line (Fig. 2a; Table S2). A more detailed analysis of the term of 'plant hormone signal transduction' revealed that most differentially expressed genes were mainly related to the auxin signaling pathway and upregulated in the *RhPMP1*-OE line, including *Auxin transporter-like protein 2* (*RhAUX2*), *Auxin-responsive protein IAA32* (*RhIAA32*), and *Small auxin-up RNA 14/15/48/20/15A* (*RhSAUR14/15/48/20/15A*; Fig. S4). To further validate the expression of these auxin signaling pathways by RT-qPCR, we found the expression levels of all of these genes were increased in *RhPMP1*-OE and reduced in the *RhPMP1*-RNAi plants (Fig. 2b). We next investigated whether RhPMP1 directly targets these auxin-related genes to regulate VB

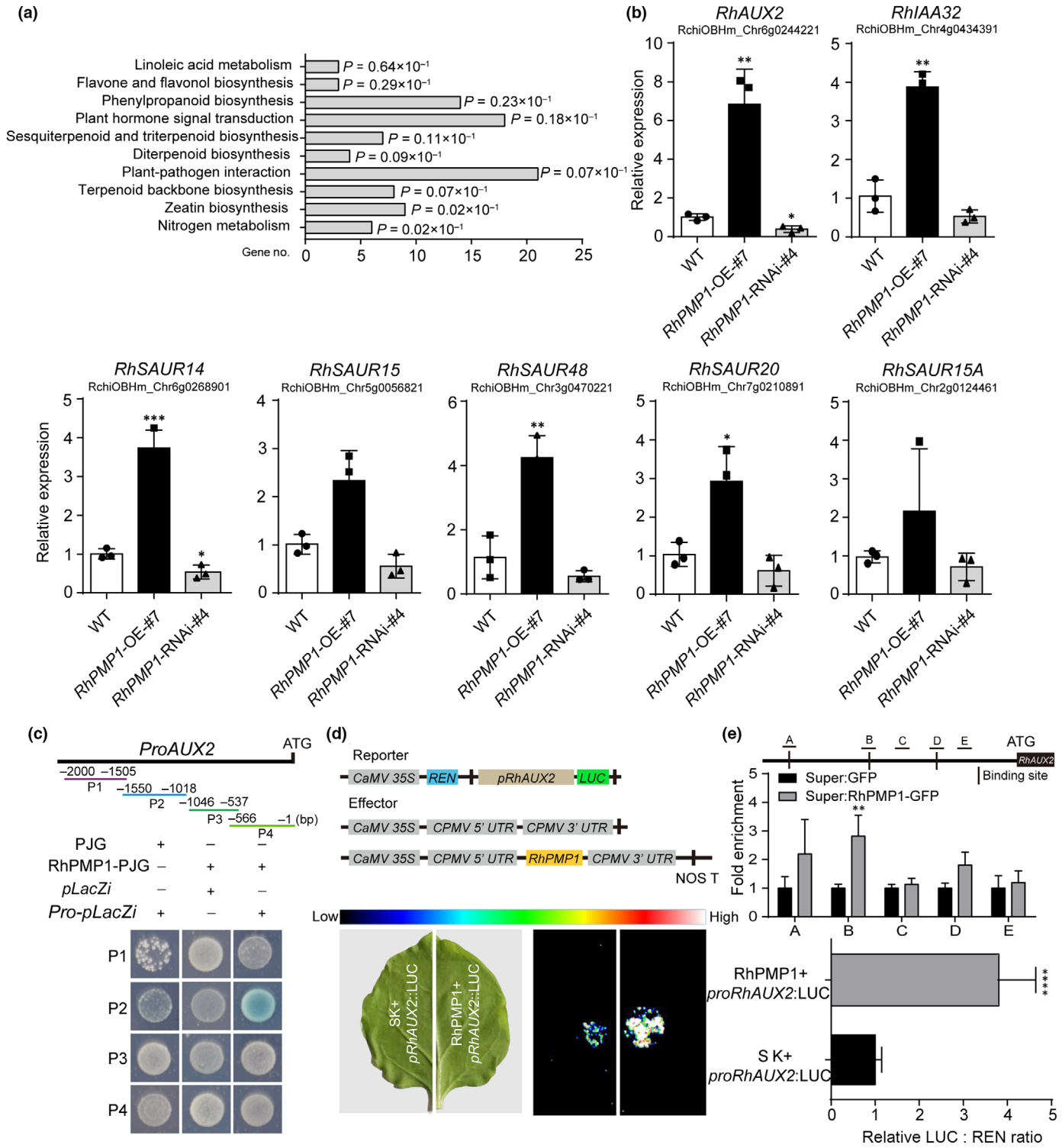

Fig. 2 *RhAUX2* is direct target of RhPMP1. (a) Significantly enriched KEGG pathways in the *RhPMP1*-OE line based on differential gene expression analysis. Enrichment of DEGs was analyzed using ClusterProfiler (3.8.1) and the corrected *P*-value cutoff was set at 0.05. (b) Expression of genes related to auxin signaling pathways in the leaf midvein of the WT and the *RhPMP1*-OE and *RhPMP1*-RNAi lines. Gene IDs: *Auxin transporter-like protein 2* (*RhAUX2*, RchiOBHm_Chr6g0244221), *Auxin-responsive protein IAA32* (*RhIAA32*, RchiOBHm_Chr4g0434391), *Small auxin-up RNA 14/15/48/20/15A* (*RhSAUR14*, RchiOBHm_Chr6g0268901; *RhSAUR15*, RchiOBHm_Chr5g0056821; *RhSAUR48*, RchiOBHm_Chr3g0470221; *RhSAUR20*, RchiOBHm_Chr7g0210891; *RhSAUR15A*, RchiOBHm_Chr2g0124461). The mean ± SD from three biological replicates is shown. Asterisks indicate statistically significant differences (Student's *t*-test: *, $P < 0.05$; **, $P < 0.01$; ***, $P < 0.001$). (c) Upper panel, diagram of the *RhAUX2* promoter. P1: −2000 to −1505 bp, P2: −1550 to −1018 bp, P3: −1046 to −537 bp, P4: −566 to −1 bp. These four fragments were used in the yeast one-hybrid assay. Lower panel, analysis of RhPMP1 binding to the *RhAUX2* promoter by yeast one-hybrid assay. PJG + *RhAUX2-pLacZi* and RhPMP1-pJG + *pLacZi* were used as negative controls. (d) Transactivation of *RhAUX2* by RhPMP1. Upper panel, diagram of the double-reporter and effector plasmids used for the dual-luciferase (*LUC*) reporter assay. Bottom panel, live imaging; leaves harboring the empty vector (SK) and the *RhAUX2* promoter were used as a negative control. Right panel, quantitative analysis; values are mean ± SD ($n = 6$). Asterisks indicate statistically significant differences (Student's *t*-test: ****, $P < 0.0001$). All experiments were independently repeated three times and representative results are shown. (e) Chromatin immunoprecipitation (ChIP)-qPCR assay showing RhPMP1 binding to the *RhAUX2* promoter *in planta*. Upper panel, schematic representation of the *RhAUX2* promoter. Black vertical lines represent the putative HD-ZIP I binding site motif (−1846 to −1839 bp, −1239 to −1248 bp, −715 to −708 bp); lines above, fragments amplified in the ChIP-qPCR analysis. A: −1910 to −1783 bp, B: −1341 to −1202 bp, C: −999 to −873 bp, D: −768 to −641 bp, E: −294 to −151 bp relative to the *RhAUX2* translation initiation codon (ATG). Cross-linked chromatin samples were extracted from *RhPMP1*-OE petals and precipitated using anti-GFP antibody. The *ProSuper::GFP* plants were used as a negative control. Values are mean ± SD. Asterisks indicate statistically significant differences (Student's *t*-test: **, $P < 0.01$).

development. Yeast one-hybrid confirmed that PhPMP1 can bind to the P2 region of *RhAUX2* promoter, but not to the *RhSAUR15* or *RhIAA32* promoters (Figs 2c, S5). We then using dual-luciferase reporter system and live imaging showed that co-infiltration of 35S:RhPMP1 effector and the *ProRhAUX2*:LUC reporter resulted in increased luciferase activity compared with empty effector (Fig. 2d). ChIP-qPCR further supported that RhPMP1 binds to the *RhAUX2* promoter *in planta* (Fig. 2e). These results demonstrated that RhPMP1 can directly bind to the *RhAUX2* promoter and activated its expression.

Considering that the activity of cambium was regulated by phytohormone, we conducted liquid chromatography–tandem mass spectrometry (LC–MS/MS) analysis the level of hormone in leaf midvein. We measured auxin (IAA), abs*cis*ic acid (ABA), jasmonic acid (JA), and salicylic acid (SA) content, among all tested phytohormones, ABA content in *RhPMP1*-OE line was similar to that in WT line and was decreased in *RhPMP1*-RNAi line. Both JA and SA content in *RhPMP1*-OE or *RhPMP1*-RNAi line was higher than that in WT line. As expected, the IAA level was significantly elevated in the *RhPMP1*-OE line but reduced in the *RhPMP1*-RNAi line (Fig. 3a–d). Next, we visualized auxin distribution in VBs by immunolocalization using an anti-indole-3-acetic acid (IAA) polyclonal antibody. Consistent with the above results, the auxin maximum was broadened and enhanced from the xylem side toward the phloem in the *RhPMP1*-OE cambium, but it was severely weakened in the *RhPMP1*-RNAi line (Figs 3e,f, S6). These results suggested that *RhPMP1* affects vascular development probably by influencing auxin biosynthesis.

TRYPTOPHAN AMINOTRANSFERASE OF ARABIDOPSIS (*TAA*) and *YUCCAs* (*YUCs*) genes encode the key enzymes responsible for auxin biosynthesis in plants (Zhao, 2018). We identified one *L-tryptophan–pyruvate aminotransferase 1* (*TAA1*), one *tryptophan aminotransferase-related protein 1* (*TAR1*), and six *YUCs* genes in the rose genome (Table S3). qRT-PCR revealed that the expression of *RhYUC3*, *RhYUC5*, and *RhYUC10* was elevated in *RhPMP1*-OE plants compared with WT. But, only *RhYUC10* expression was repressed in *RhPMP1*-RNAi plants (Fig. S7), suggesting that *RhPMP1* may promote auxin accumulation through enhancing *RhYUC10* expression.

To test whether RhPMP1 directly binds to the promoter of *RhYUC2* and *RhYUC10*, we found the conserved HD-ZIP I TF binding site 'CAATNATTG' in the *RhYUC2* and *RhYUC10* promoters. Yeast one-hybrid assay showed that PhPMP1 bound to the proximal promoter of *RhYUC10*, but not to that of *RhYUC2* (Figs 4a, S5c). Electrophoretic mobility shift assay (EMSA) validated the binding of RhPMP1 with the 'CAATNATTG' *cis*-element of the *RhYUC10* promoter *in vitro* (Fig. 4b). Chromatin immunoprecipitation (ChIP)-qPCR further supported that RhPMP1 binds to the proximal promoter of *RhYUC10 in planta* (Fig. 4c). A quantitative luciferase activity assay and live imaging of *Nicotiana benthamiana* leaves co-transformed with the *35S:RhPMP1* effector and the *ProRhYUC10*: *LUC* reporter confirmed that RhPMP1 activates *RhYUC10* expression (Fig. 4d). These results indicated that RhPMP1 binds to and activates the RhYUC10 promoter.

Considering that auxin is unevenly distributed in VBs, we explored the expression pattern of *RhYUC10* and *RhAUX2* using *in situ* hybridization. *RhYUC10* expression was pronouncedly elevated in the *RhPMP1*-OE line compared with the WT, while it was attenuated in the *RhPMP1*-RNAi line. *RhYUC10* transcripts were highly concentrated in the region of the cambium adjacent to the xylem (Fig. 5a), overlapping with the maximum of auxin concentration. Moreover, the *RhAUX2* expression pattern was similar to that of *RhYUC10* (Fig. 5b). These results suggested that RhPMP1 controls local auxin biosynthesis and accumulation in the region of the cambium facing the xylem by specifically activating *RhYUC10* and *RhAUX2*.

WUSCHEL-RELATED HOMEOBOX 4 (*WOX4*) and *AUXIN RESPONSE FACTOR 5* (*ARF5*) are key players in auxin-promoted vascular cambium activity, and *ARF5* also promotes xylem differentiation (Suer *et al.*, 2011; Kucukoglu *et al.*, 2017; Tang *et al.*, 2022). Therefore, we detected the *RhWOX4* and *RhARF5* expression patterns in the WT and the *RhPMP1*-OE

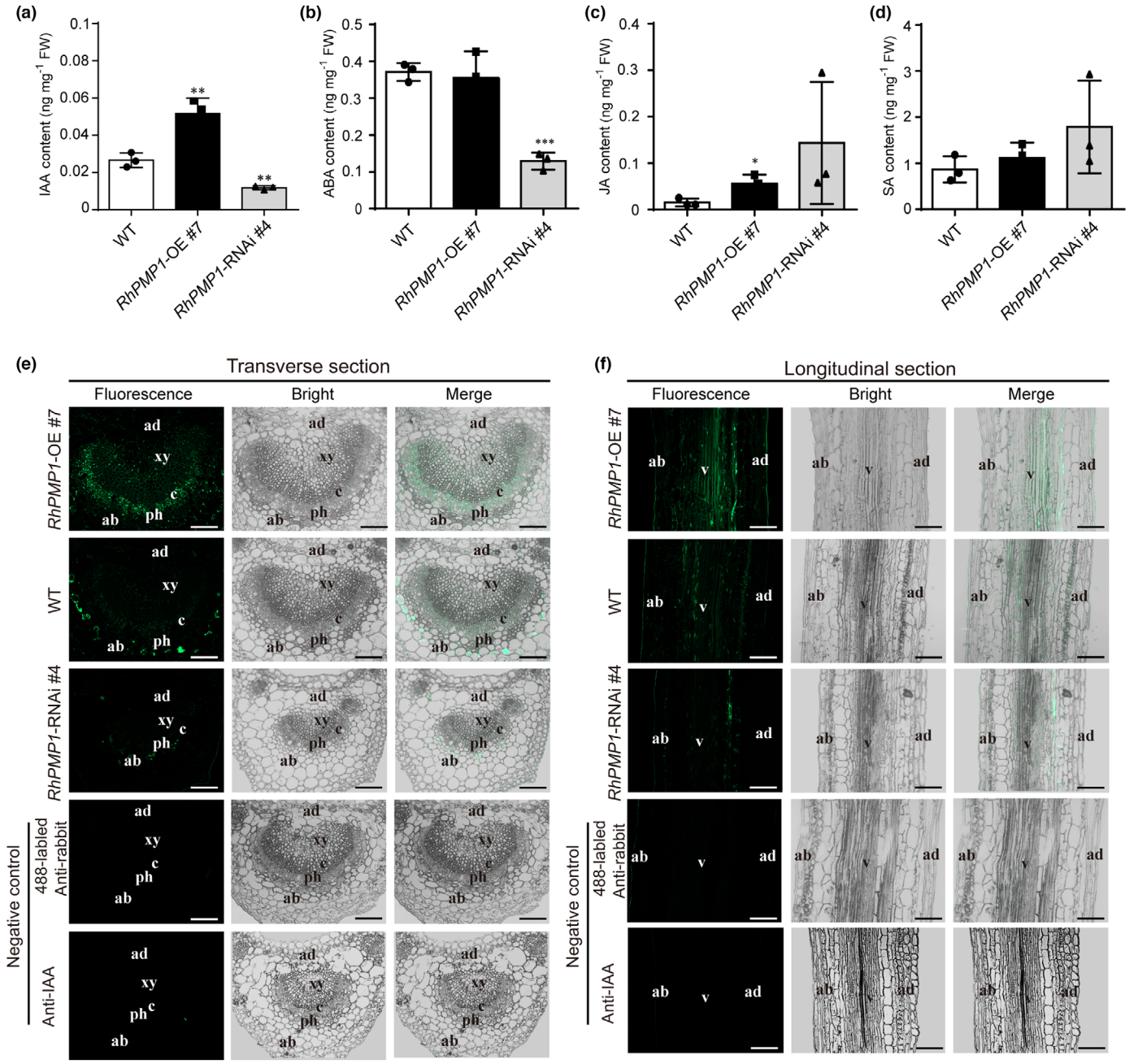

Fig. 3 Hormone levels in WT, *RhPMP1*-OE, and *RhPMP1*-RNAi lines transgenic plants. (a–d) Hormone contents in the leaf midvein of the WT and the *RhPMP1*-OE #7 and *RhPMP1*-RNAi #4 lines. Indole acetic acid (IAA) (a), ABA (b), JA (c), and SA (d) were determined using liquid chromatography–tandem mass spectrometry. The mean ± SD from three biological replicates is shown with at least 10 samples per replicate. Asterisks indicate statistically significant differences (Student's *t*-test: *, $P < 0.05$; **, $P < 0.01$; ***, $P < 0.001$). (e, f) Immunolocalization of IAA in transverse sections (d) and longitudinal sections (e) of the WT and the *RhPMP1*-OE #7 and *RhPMP1*-RNAi #4 lines. Immunofluorescence assays were conducted using anti-IAA antibody and ABflo™ 488-conjugated goat anti-rabbit IgG antibody. The sections of stem not incubated with the primary anti-auxin antibody were used as negative controls. ad, adaxial; ab, abaxial; xy, xylem; ph, phloem; c, cambium; v, vascular bundle. Bars, 20 µm. All experiments were repeated three times and representative results are shown.

and *RhPMP1*-RNAi lines. *In situ* hybridization showed that *RhWOX4* and *RhARF5* were upregulated in *RhPMP1*-OE vascular cells compared with WT plants, while these genes were suppressed in vascular cells of *RhPMP1*-RNAi plants (Fig. 5c,d), supporting that the RhPMP1-RhYUC10 module promotes cambium activity via an auxin-dependent pathway.

RhPMP1 is required for ethylene-induced secondary vascular cell division

To further verify the role of *RhPMP1* in ethylene-induced vascular cell division, we compared VB development in WT and *RhPMP1*-RNAi plants in response to 1-aminocyclopropane-1-

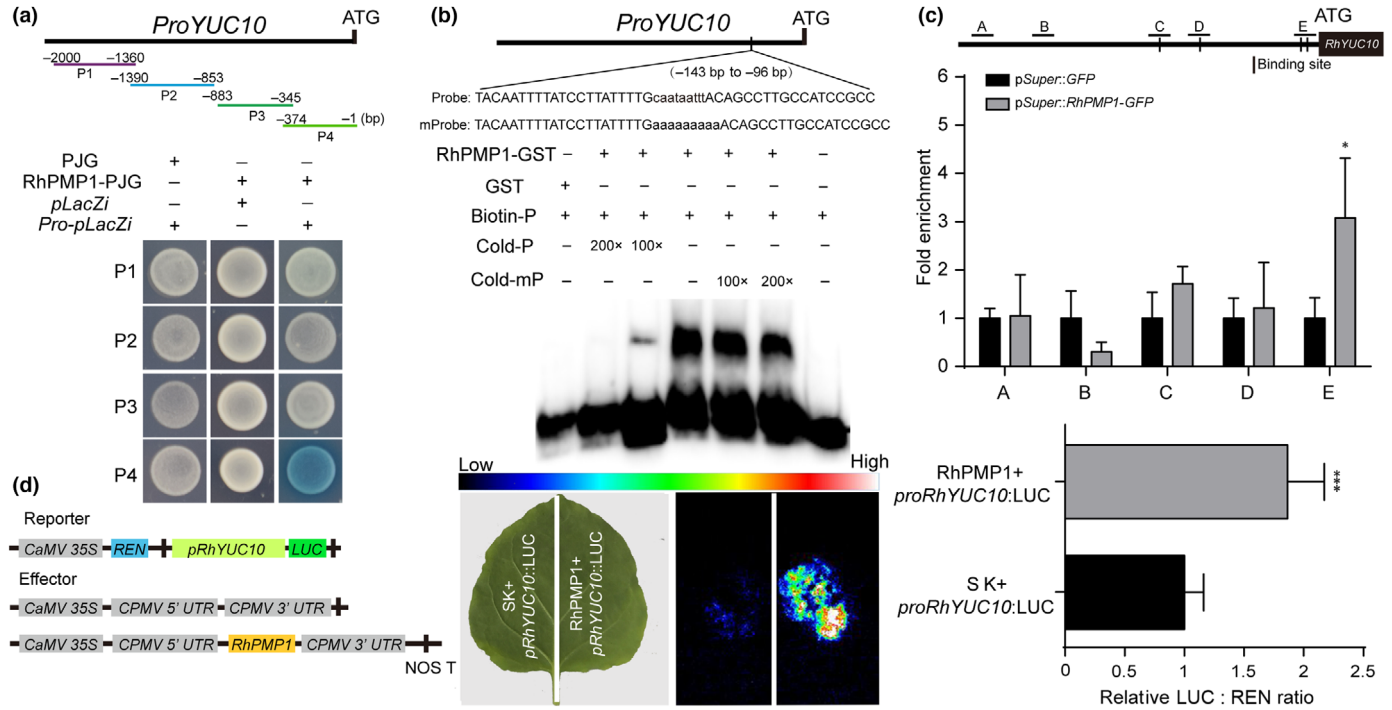

Fig. 4 *RhYUC10* is a direct target of RhPMP1. (a) Upper panel, diagram of the *RhYUC10* promoter. P1: −2000 to −1360 bp, P2: −1390 to −853 bp, P3: −883 to −345 bp, P4: −374 to −1 bp. These four fragments were used in the yeast one-hybrid assay. Lower panel, analysis of RhPMP1 binding to the *RhYUC10* promoter by yeast one-hybrid assay. PJG + *RhYUC10-pLacZi* and RhPMP1-pJG + *pLacZi* were used as negative controls. (b) Electrophoretic mobility shift assay (EMSA) analysis of RhPMP1 binding to the HD-ZIP I motif in the *RhYUC10* promoter. The fragment of the *RhYUC10* promoter containing the RhPMP1 binding site from −143 to −96 bp was used as a probe. Non-labeled probe at 100- or 200-fold was used for the competition test. Mutant probe and GST protein were used as negative controls. (c) ChIP-qPCR assay showing RhPMP1 binding to the *RhYUC10* promoter *in planta*. Upper panel, schematic representation of the *RhYUC10* promoter. Black vertical lines, the putative HD-ZIP I binding site motif (−1214 to −1203 bp, −851 to −841 bp, −246 to −237 bp, −123 to −114 bp); lines above, the fragments amplified in the ChIP-qPCR analysis. A: −1957 to −1828 bp, B: −1612 to −1489 bp, C: −1271 to −1149 bp, D: −924 to −811 bp, E: −153 to −109 bp relative to the *RhYUC10* translation initiation codon (ATG). Cross-linked chromatin samples were extracted from *RhPMP1*-OE petals and precipitated using anti-GFP antibody. The *ProSuper::GFP* plants were used as a negative control. Values are mean ± SD. Asterisks indicate statistically significant differences (Student's *t*-test: *, $P < 0.05$). (d) Transactivation of *RhYUC10* by RhPMP1. Left panel, diagram of the double-reporter and effector plasmids for the dual-luciferase (*LUC*) reporter assay. Middle panel, live imaging; leaves harboring the empty vector (SK) and the *RhYUC10* promoter were used as a negative control. Right panel, quantitative analysis; values are mean ± SD ($n = 6$). Asterisks indicate statistically significant differences (Student's *t*-test: ***, $P < 0.001$). All experiments were independently repeated three times, and representative results are shown.

carboxylic acid (ACC), the precursor of ethylene. In ACC treatment, the stem diameter of WT plants increased significantly, but of *RhPMP1*-RNAi plants increased slightly (Fig. S8a–d), consistent with a previous report in poplar (Love *et al.*, 2009). Pith and cortex cells were significantly larger in ACC-treated WT plants than in untreated WT plants (Fig. S8e,f). The vascular size of *RhPMP1*-RNAi plants was significantly smaller than that in WT plants, especially in ACC-treated *RhPMP1*-RNAi plants (Fig. 6a–d). In addition, ACC elevated xylem cell number and the size of the xylem cells in WT plants (Fig. 6e,f). These results suggested that RhPMP1 is dispensable for ethylene-induced vascular cambium activity.

Moreover, as expected, ACC treatment pronouncedly induced *RhYUC10* and *RhAUX2* expression in the cambium cells facing the xylem (Fig. 7a–c) and consequently enhanced the auxin maximum in the same region. In the *RhPMP1*-RNAi, however, ACC failed to induce *RhYUC10* and *RhAUX2* expression and thus barely increased the auxin level in the vascular cambium (Figs 7d,e, S9), indicating that ethylene promotes cambium stem cell activity by directly stimulating local auxin biosynthesis and transport.

Discussion

Apical growth of plants, for example, to harvest light, requires physical support of aerial organs and transport of water and nutrients. The vascular cambium provides the potency to grow radially along the primary axes to provide additional support to the plant and expand the capacity of the vascular system. This so-called secondary growth is tightly coordinated with primary growth. Auxin is a critical phytohormone for coordinating primary and secondary growth via modulating the activity of cambial stem cells. Removing the auxin source, such as the shoot apex, halts secondary growth, while exogenous auxin application restores some aspects of secondary growth (Sundberg & Uggla, 1998, Björklund *et al.*, 2007, Agusti *et al.*, 2011, Johnsson *et al.*, 2019). Therefore, shoot apex-derived auxin is considered the major regulator of cambial activity and radial growth.

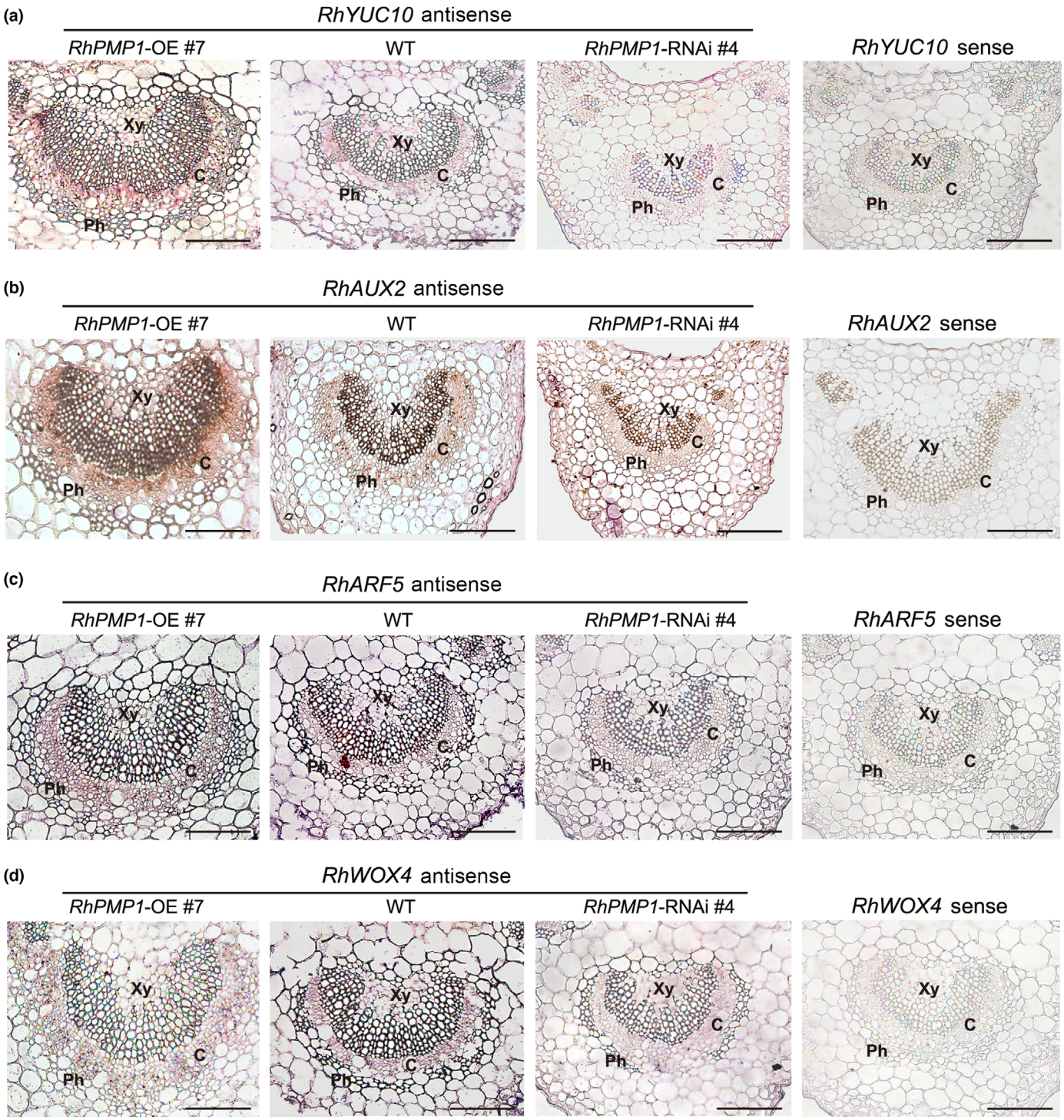

Fig. 5 Expression pattern of *RhYUC10*, *RhAUX2*, *RhARF5*, and *RhWOX4* in leaf veins of WT, *RhPMP1*-OE, and *RhPMP1*-RNAi lines. *In situ* hybridization of *RhYUC10* (RchiOBHm_Chr5g0016501) (a), *RhAUX2* (RchiOBHm_Chr6g0244221) (b), *RhARF5* (RchiOBHm_Chr6g0302551) (c), and *RhWOX4* (RchiOBHm_Chr6g0308351) (d) in leaf midveins of the WT and the *RhPMP1*-OE and *RhPMP1*-RNAi lines. Sense probes were hybridized as the negative controls. Xy, xylem; Ph, phloem; c, cambium. Bars, 100 µm. All experiments were repeated three times and representative results are shown.

In this study, we found that local auxin biosynthesis in certain cambial stem cells might be indispensable to maintain cambial activity and radial growth. Knockdown of an ethylene-induced HD-ZIP I transcription factor gene, *RhPMP1*, resulted in defects in cambial activity and, consequently, xylem and phloem development due to decreased auxin levels in cambium stem cells. We demonstrated that RhPMP1 transcriptionally activates the auxin biosynthetic gene *RhYUC10*. Moreover, exogenous application of the ethylene precursor ACC stimulated cambium stem cell activity by enhancing local auxin biosynthesis. Notably,

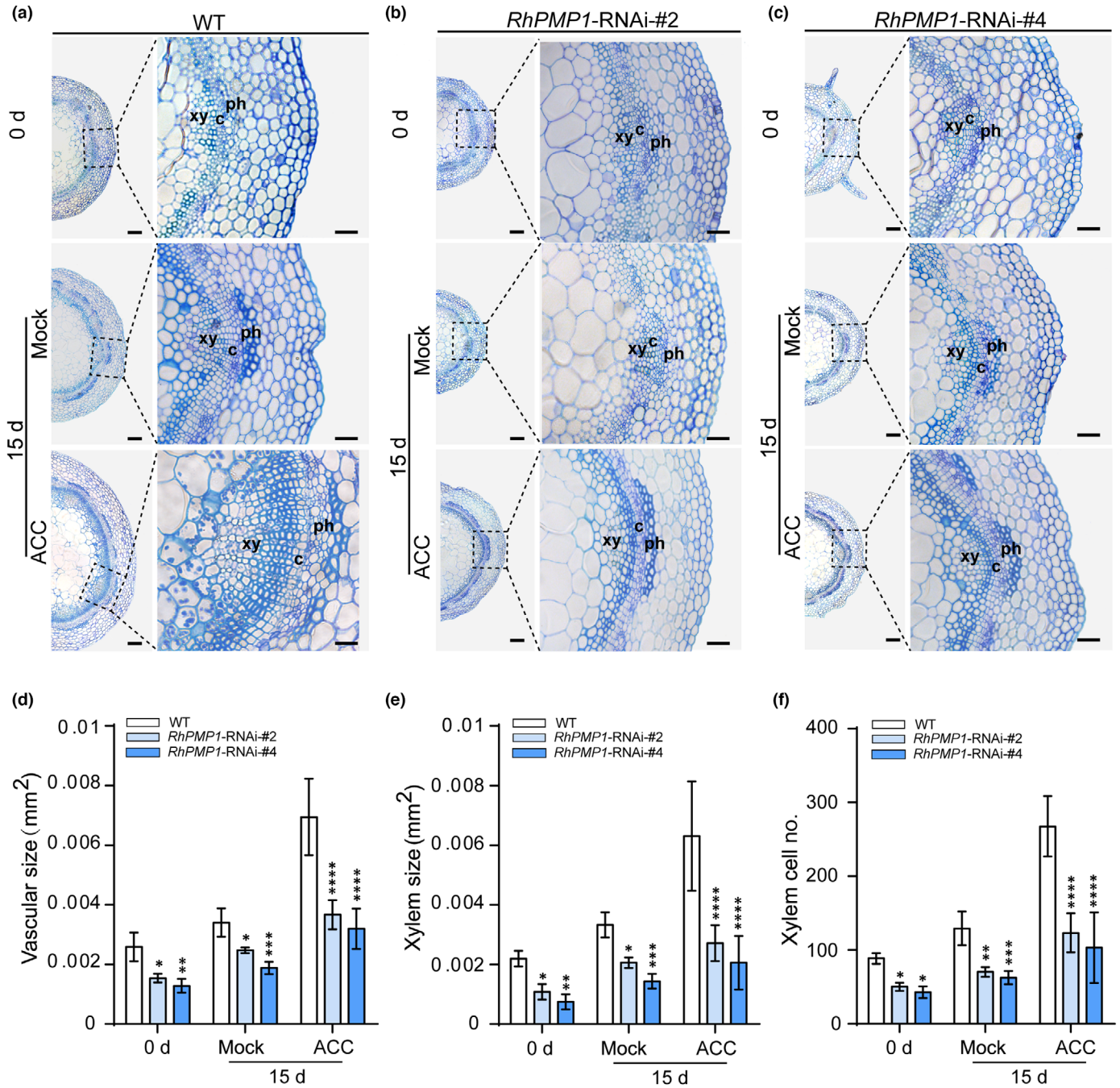

Fig. 6 Histological analysis of stem vascular of WT and *RhPMP1*-RNAi lines in response to ACC treatment. (a–c) Histological analysis of stems of WT (a), *RhPMP1*-RNAi-#2 (b), and *RhPMP1*-RNAi-#4 (c) tissue-cultured seedlings. The plants were proliferated for 1 month and subjected to mock or ACC (100 μM) treatment for 15 d; then, the first newly formed node (stem) was sampled. The right panels show the enlarged areas marked in left panels. Bars: 50 and 20 μm for left and right panels, respectively. ph, phloem; xy, xylem; c, cambium. (d–f) Size of the vasculature (c), size of the xylem (d), and xylem cell number (e) of the WT and the *RhPMP1*-RNAi (#2 and #4) line. Values are mean ± SD ($n = 5$). Asterisks indicate statistically significant differences (Student's *t*-test: *, $P < 0.05$; **, $P < 0.01$; ***, $P < 0.001$; ****, $P < 0.0001$). All experiments were repeated three times and representative results are shown.

ethylene-stimulated local auxin biosynthesis was most pronounced in the cambium stem cells adjacent to the xylem, and this region has been identified as the stem cell organizer of vascular cambium (Smetana *et al.*, 2019). Therefore, we considered that ethylene has a vital role in defining the stem cell organizer of vascular cambium by modulating local auxin biosynthesis. Ethylene also modulates cell division in the QC in the stem cell niche of roots in Arabidopsis (Ortega-Martinez *et al.*, 2007). Cell division in the QC is higher in the ethylene-overproducing *eto1* mutant than in the WT, but is lower in the ethylene-insensitive

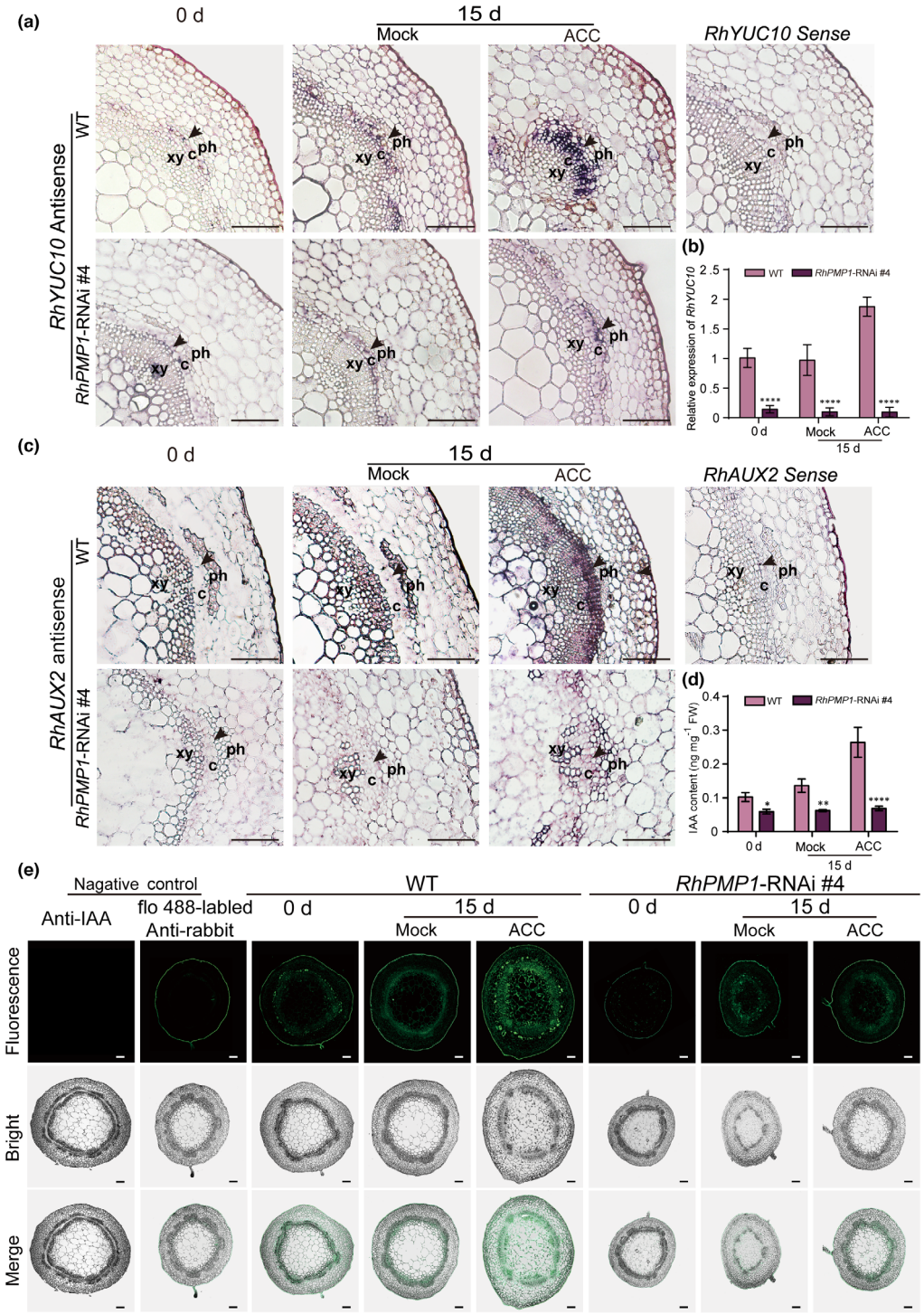

Fig. 7 Expression pattern of *RhYUC10* and *RhAUX2*, and auxin level in stem of WT and *RhPMP1*-RNAi plants in response to ACC treatment. (a, c) *In situ* hybridization of *RhYUC10* (a) and *RhAUX2* (c) of WT and *RhPMP1*-RNAi tissue-cultured seedlings. The plants were proliferated for 1 month and subjected to mock or ACC (100 μM) treatment for 15 d; then, the first newly formed internode (stem) was sampled. The sense *RhYUC10* probe was hybridized as a negative control. The arrowheads indicate the signal of *RhYUC10*. Bars, 50 μm. ph, phloem; xy, xylem; c, cambium. (b) RT-qPCR of *RhYUC10* in the WT and the *RhPMP1*-RNAi line in response to ACC treatment. Values are mean ± SD ($n = 3$). Asterisks indicate statistically significant differences (Student's *t*-test: ****, $P < 0.0001$). (d) Indole acetic acid (IAA) contents in the stem of the WT and the *RhPMP1*-RNAi #4 lines. IAA was determined using liquid chromatography–tandem mass spectrometry. The mean ± SD from three biological replicates is shown. Asterisks indicate statistically significant differences (Student's *t*-test: *, $P < 0.05$; **, $P < 0.01$; ****, $P < 0.0001$). (e) Immunolocalization of IAA of WT and *RhPMP1*-RNAi #4 tissue-cultured seedlings. The plants were proliferated for 1 month and subjected to mock or ACC (100 μM) treatment for 15 d; then, the first newly formed internode was sampled. Immunofluorescence assays used anti-IAA antibody and ABflo™ 488-conjugated goat anti-rabbit IgG. The section of stem incubated with IgG was used as a negative control. Bars, 20 μm. All experiments were repeated three times and representative results are shown.

ethylene insensitive 2 (*ein2*) mutant. Blocking ethylene biosynthesis by aminoethoxyvinylglycine weakens cell division activity in the QC in roots as well (Ortega-Martinez *et al.*, 2007). However, treatment with naphthaleneacetic acid (NAA), a synthetic auxin, does not stimulate cell division in the QC. One explanation for this is that auxin is not required for ethylene-induced cell division in the QC. Auxin and ethylene also coordinately regulate root growth. In Arabidopsis, *weak ethylene insensitive8* (*wei8*) identified as a root-specific ethylene insensitivity mutant (Stepanova *et al.*, 2008). Ethylene inhibits root growth by accelerating auxin biosynthesis (*WEI2*/*ASA1* and *WEI7*/*ASB1*) and auxin transport (*AUX1*; Swarup *et al.*, 2007). Apical-derived auxin activates Auxin receptor (*TIR*) and *AUX*/*IAA*, and inhibits root cell elongation (Růžička *et al.*, 2007). Meanwhile, it is found that EIN3 activates auxin biosynthetic genes (*WEI2*, *WEI7*, *TAA1*, and *TAR2*), in turn, IAA is also can be enhance EIN3 stability, thus forming a positive feedback loop between ethylene signaling and auxin biosynthesis in the regulation of root elongation (He *et al.*, 2011). Enriching the stem cell niche with endogenous ethylene is crucial for stem cell maintenance through a AGL22-CLV1/2-WUS pathway in Arabidopsis shoots (Zeng *et al.*, 2021). These studies combined with our results indicate that ethylene regulates stem cell activity in different meristematic tissues, that is, the root apical meristem (RAM), shoot apical meristem (SAM), and cambium, through different pathways.

Rice (*Oryza sativa*) plants grown in compacted soil accumulate ethylene in roots, which activates *OsYUC8* via the ethylene-induced transcription factor *ETHYLENE INSENSITIVE 3-Like 1* (*OsEIL1*) in inner tissues of root tips. Moreover, an auxin influx carrier, OsAUX1, facilitates shootward auxin transport to epidermal cells of the elongation zone from the root apex, consequently inhibiting root epidermal cell elongation, and thus root elongation (Huang *et al.*, 2022). Intriguingly, RhPMP1 also directly targeted and activated *RhAUX2*, encoding a typical auxin influx carrier, in the cambium region, whose expression mostly overlapped with the auxin maximum. Therefore, ethylene simultaneously stimulates local auxin biosynthesis (*RhYUC10*), polar auxin transport (*RhAUX2*), and the regulators of auxin-promoted vascular cambium activity (*RhWOX4*&*RhARF5*) to establish the auxin maximum, then promoted cambium activity (Fig. S10). An interesting question is whether ethylene-induced RhAUX2 is involved in transporting shoot apex-derived auxin to the cambium cells. Moreover, it remains to be investigated how the distribution/redistribution of shoot apex-derived auxin and ethylene-induced local auxin biosynthesis are coordinated in cambium stem cells.

In addition, crosstalk of ethylene and auxin has been documented in regulation of development of roots. In Arabidopsis, *ethylene response factor1* (*ERF1*) inhibits primary root elongation through upregulating *ASA1*, a rate-limiting enzyme in tryptophan biosynthesis (Mao *et al.*, 2016). Ethylene transcription factor *OsEIL1* activates *OsYUC8*/*REIN7* to inhibit primary root elongation of rice (Qin *et al.*, 2017). Since *RhPMP1* can enhance local biosynthesis of auxin in cambial cells, whether *RhPMP1* is involved in regulation of root development deserves further investigation.

Acknowledgements

This work was supported by the earmarked fund for CARS-23, the National Natural Science Foundation of China (31872148 & 31902056), the Construction of Beijing Science and Technology Innovation and Service Capacity in Top Subjects (CEFF-PXM2019_014207_000032), and the 111 Project (B17043). We thank Dr Zhizhong Gong (China Agricultural University) for providing the *pSuper*1300 vector and Dr Yin Bao (Tangshan Normal University) for generous help in generation of transgenic rose plants. We thank PlantScribe (www.plantscribe.com) for careful editing of this article.

Competing interests

None declared.

Author contributions

NM designed the research. QY, CC, XZ, CY and YZ performed the experiments. YL, YH, HZ, QW, HW and TMAS provided the technical support. C-ZJ, S-SG and JG provided the conceptual advices. QY, CC, XZ and NM analyzed the data analysis. QY, CC and NM wrote the manuscript.

ORCID

Chenxia Cheng https://orcid.org/0000-0002-6375-9597
Su-Sheng Gan https://orcid.org/0000-0002-9687-2780
Junping Gao https://orcid.org/0000-0002-9285-2539
Cai-Zhong Jiang https://orcid.org/0000-0002-5972-7963
Nan Ma https://orcid.org/0000-0002-2176-3133
Tarek M. A. Soliman https://orcid.org/0000-0002-5082-2497
Qin Yu https://orcid.org/0000-0002-0619-450X

Data availability

The high-throughput sequencing datasets generated in this study have been deposited in the Sequence Read Archive (SRA) under the accession no SRA: PRJNA906463. The data that support the findings of this study are available in the Supporting Information.

References

Agusti J, Herold S, Schwarz M, Sanchez P, Ljung K, Dun EA, Brewer PB, Beveridge CA, Sieberer T, Sehr EM *et al.* 2011. Strigolactone signaling is required for auxin-dependent stimulation of secondary growth in plants. *Proceedings of the National Academy of Sciences, USA* **108**: 20242–20247.

Björklund S, Antti H, Uddestrand I, Moritz T, Sundberg B. 2007. Cross-talk between gibberellin and auxin in development of *Populus* wood: gibberellin stimulates polar auxin transport and has a common transcriptome with auxin. *The Plant Journal* **52**: 499–511.

Cheng C, Yu Q, Wang Y, Wang H, Dong Y, Ji Y, Zhou X, Li Y, Jiang C, Gan S *et al.* 2021. Ethylene-regulated asymmetric growth of the petal base promotes flower opening in rose (*Rosa hybrida*). *Plant Cell* **33**: 1229–1251.

Etchells JP, Provost CM, Turner SR. 2012. Plant vascular cell division is maintained by an interaction between PXY and ethylene signalling. *PLoS Genetics* **8**: e1002997.

He W, Brumos J, Li H, Ji Y, Ke M, Gong X, Zeng Q, Li W, Zhang X, An F *et al.* 2011. A small-molecule screen identifies L-kynurenine as a competitive inhibitor of TAA1/TAR activity in ethylene-directed auxin biosynthesis and root growth in Arabidopsis. *Plant Cell* **23**: 3944–3960.

Hemerly AS, Ferreira P, de Almeida Engler J, Van Montagu M, Engler G, Inzé D. 1993. cdc2a expression in Arabidopsis is linked with competence for cell division. *Plant Cell* **5**: 1711–1723.

Hirakawa Y, Kondo Y, Fukuda H. 2010. TDIF peptide signaling regulates vascular stem cell proliferation via the WOX4 homeobox gene in Arabidopsis. *Plant Cell* **22**: 2618–2629.

Hu B, Zhang G, Liu W, Shi J, Wang H, Qi M, Li J, Qin P, Ruan Y, Huang H *et al.* 2016. Divergent regeneration-competent cells adopt a common mechanism for callus initiation in angiosperms. *Regeneration* **4**: 132–139.

Huang G, Kilic A, Karady M, Zhang J, Mehra P, Song X, Sturrock CJ, Zhu W, Qin H, Hartman S *et al.* 2022. Ethylene inhibits rice root elongation in compacted soil via ABA- and auxin-mediated mechanisms. *Proceedings of the National Academy of Sciences, USA* **119**: e2201072119.

Hur YS, Um JH, Kim S, Kim K, Park HJ, Lim JS, Kim WY, Jun SE, Yoon EK, Lim J *et al.* 2015. *Arabidopsis thaliana* homeobox 12 (ATHB12), a homeodomain-leucine zipper protein, regulates leaf growth by promoting cell expansion and endoreduplication. *New Phytologist* **205**: 316–328.

Johnsson C, Jin X, Xue W, Dubreuil C, Lezhneva L, Fischer U. 2019. The plant hormone auxin directs timing of xylem development by inhibition of secondary cell wall deposition through repression of secondary wall NAC-domain transcription factors. *Physiologia Plantarum* **165**: 673–689.

Kucukoglu M, Nilsson J, Bo Z, Chaabouni S, Nilsson O. 2017. *WUSCHEL-RELATED HOMEOBOX4* (*WOX4*)-like genes regulate cambial cell division activity and secondary growth in *Populus* trees. *New Phytologist* **215**: 642–657.

Liang Y, Jiang C, Liu Y, Gao Y, Lu J, Aiwaili P, Fei Z, Jiang C-Z, Hong B, Ma C *et al.* 2020. Auxin regulates sucrose transport to repress petal abscission in rose (*Rosa hybrida*). *Plant Cell* **32**: 3485–3499.

Little C, Savidge RA. 1987. The role of plant growth regulators in forest tree cambial growth. *Plant Growth Regulation* **6**: 137–169.

Love J, Björklund S, Vahala J, Hertzberg M, Kangasjärvi J, Sundberg B. 2009. Ethylene is an endogenous stimulator of cell division in the cambial meristem of *Populus. Proceedings of the National Academy of Sciences, USA* **106**: 5984–5989.

Lucas WJ, Groover A, Lichtenberger R, Furuta K, Yadav SR, Helariutta Y, He XQ, Fukuda H, Kang J, Brady SM *et al.* 2013. The plant vascular system: evolution, development and functions. *Journal of Integrative Plant Biology* **55**: 294–388.

Mao JL, Miao ZQ, Wang Z, Yu LH, Cai XT, Xiang CB. 2016. Arabidopsis ERF1 mediates cross-talk between ethylene and auxin biosynthesis during primary root elongation by regulating *ASA1* expression. *PLoS Genetics* **12**: e1005760.

Moreno JE, Romani F, Chan RL. 2018. *Arabidopsis thaliana* homeodomain-leucine zipper type I transcription factors contribute to control leaf venation patterning. *Plant Signaling & Behavior* **13**: e1448334.

Nie J, Shan N, Liu H, Yao X, Sui X. 2021. Transcriptional control of local auxin distribution by the CsDFB1-CsPHB module regulates floral organogenesis in cucumber. *Proceedings of the National Academy of Sciences, USA* **118**: e2023942118.

Oles V, Panchenko A, Smertenko A. 2017. Modeling hormonal control of cambium proliferation. *PLoS ONE* **12**: e0171927.

Ortega-Martinez O, Pernas M, Carol RJ, Dolan L. 2007. Ethylene modulates stem cell division in the *Arabidopsis thaliana* root. *Science* **317**: 507–510.

Qin H, Zhang Z, Wang J, Chen X, Wei P, Huang R. 2017. The activation of OsEIL1 on *YUC8* transcription and auxin biosynthesis is required for ethylene-inhibited root elongation in rice early seedling development. *PLoS Genetics* **13**: e1006955.

Růžička K, Ljung K, Vanneste S, Podhorská R, Beeckman T, Friml JI, Benková E. 2007. Ethylene regulates root growth through effects on auxin biosynthesis and transport-dependent auxin distribution. *Plant Cell* **19**: 2197–2212.

Seyfferth C, Wessels B, Jokipii-Lukkari S, Sundberg B, Delhomme N, Felten J, Tuominen H. 2018. Ethylene-related gene expression networks in wood formation. *Frontiers in Plant Science* **9**: 272.

Seyfferth C, Wessels BA, Gorzsas A, Love JW, Ruggeberg M, Delhomme N, Vain T, Antos K, Tuominen H, Sundberg B *et al.* 2019. Ethylene signaling is required for fully functional tension wood in hybrid aspen. *Frontiers in Plant Science* **10**: 1101.

Smetana O, Mäkilä R, Lyu M, Amiryousefi A, Rodriguez FS, Wu MF, Sole-Gil A, Gavarron ML, Siligato R, Miyashima S. 2019. High levels of auxin signalling define the stem-cell organizer of the vascular cambium. *Nature* **565**: 485–489.

Stepanova AN, Robertson-Hoyt J, Yun J, Benavente LM, Xie DY, Dolezal K, Schlereth A, Jurgens G, Alonso JM. 2008. TAA1-mediated auxin biosynthesis is essential for hormone crosstalk and plant development. *Cell* **133**: 177–191.

Suer S, Agusti J, Sanchez P, Schwarz M, Greb T. 2011. *WOX4* imparts auxin responsiveness to cambium cells in *Arabidopsis. Plant Cell* **23**: 3247–3259.

Sugimoto K, Jiao YL, Meyerowitz EM. 2010. Arabidopsis regeneration from multiple tissues occurs via a root development pathway. *Developmental Cell* **18**: 463–471.

Sundberg B, Uggla C. 1998. Origin and dynamics of indoleacetic acid under polar transport in *Pinus sylvestris. Physiologia Plantarum* **104**: 22–29.

Swarup R, Perry P, Hagenbeek D, Straeten D, Beemster G, Sandberg G, Bhalerao R, Bennett L. 2007. Ethylene upregulates auxin biosynthesis in Arabidopsis seedlings to enhance inhibition of root cell elongation. *Plant Cell* **19**: 2186–2196.

Tang X, Wang C, Chai G, Wang D, Xu H, Liu Y, He G, Liu S, Zhang Y, Kong Y. 2022. Ubiquitinated DA1 negatively regulates vascular cambium activity through modulating the stability of WOX4 in *Populus. Plant Cell* **34**: 3364–3382.

Vahala J, Felten J, Love J, Gorzsas A, Gerber L, Lamminmaki A, Kangasjarvi J, Sundberg B. 2013. A genome-wide screen for ethylene-induced ethylene response factors (ERFs) in hybrid aspen stem identifies *ERF* genes that modify stem growth and wood properties. *New Phytologist* **200**: 511–522.

Yang S, Wang S, Li S, Du Q, Qi L, Wang W, Chen J, Wang H. 2020. Activation of ACS7 in Arabidopsis affects vascular development and demonstrates a link between ethylene synthesis and cambial activity. *Journal of Experimental Botany* **71**: 7160–7170.

Zeng J, Li X, Ge Q, Dong Z, Luo L, Tian Z, Zhao Z. 2021. Endogenous stress-related signal directs shoot stem cell fate in *Arabidopsis thaliana. Nature Plants* **7**: 1276–1287.

Zhao Y. 2018. Essential roles of local auxin biosynthesis in plant development and in adaptation to environmental changes. *Annual Review of Plant Biology.* **69**: 417–435.

Supporting Information

Additional Supporting Information may be found online in the Supporting Information section at the end of the article.

Fig. S1 Transactivation activity of the *RhPMP1* promoter in the transgenic *ProRhPMP1*: *GUS* Arabidopsis plants.

Fig. S2 Identification of *RhPMP1*-OE lines.

Fig. S3 Phenotypic analysis of petal midvein in WT and *RhPMP1* transgenic plants.

Fig. S4 Heatmap analysis of plant hormone signaling genes differentially expressed between WT and *RhPMP1*-OE plants.

Fig. S5 Validation of the potential targets of RhPMP1.

Fig. S6 Immunolocalization of IAA in WT and *RhPMP1* transgenic plants.

Fig. S7 RhPMP1 regulates the expression of auxin biosynthetic genes.

Fig. S8 Histological analysis of stem of WT and *RhPMP1*-RNAi lines in response to ACC treatment.

Fig. S9 Different repeats of immunolocalization of IAA in stems of WT and *RhPMP1*-RNAi plants in response to ACC treatment.

Fig. S10 Model of how ethylene governs cambium stem cell activity.

Table S1 List of primers used.

Table S2 Differentially expressed genes identified in the *RhPMP1*-OE vs WT plants by RNA-Seq.

Table S3 Auxin biosynthetic genes from *Rosa chinensis* 'Old Blush' genome.

Please note: Wiley is not responsible for the content or functionality of any Supporting Information supplied by the authors. Any queries (other than missing material) should be directed to the *New Phytologist* Central Office.